Volume 19 | Number 11 | 21 March 2017 | Pages 1441–1572

CrystEngComm

rsc.li/crystengcomm

ROYAL SOCIETY OF CHEMISTRY

PAPER

Xing Duan, Guodong Qian *et al.*

A novel methoxy-decorated metal–organic framework exhibiting high acetylene and carbon dioxide storage capacities

CrystEngComm

PAPER

View Article Online
View Journal | View Issue

Cite this: *CrystEngComm*, 2017, **19**, 1464

A novel methoxy-decorated metal–organic framework exhibiting high acetylene and carbon dioxide storage capacities†

Xing Duan,*[a] Yuanjing Cui,[b] Yu Yang[b] and Guodong Qian*[b]

Received 2nd November 2016,
Accepted 28th December 2016

DOI: 10.1039/c6ce02291j

www.rsc.org/crystengcomm

A methoxy-decorated novel metal–organic framework (MOF), Cu_2(DTPD) (**ZJU-12**, H_4DTPD = 5,5′-(2,6-dimethoxynaphthalene-1,5-diyl)diisophthalic acid) with optimized pore space and open metal sites, was solvothermally synthesized and structurally characterized. The activated **ZJU-12a** displays a moderately high BET (Brunauer–Emmett–Teller) surface area of 2316 $m^2\ g^{-1}$. Due to the pore size of the crystal being consistent with the molecular size and kinetic diameters of C_2H_2 and CO_2, **ZJU-12a** exhibits a high C_2H_2 storage capacity of 244 $cm^3\ g^{-1}$ and CO_2 capture capacity of 134 $cm^3\ g^{-1}$ at room temperature.

Introduction

Over the past few decades, metal organic frameworks (MOFs), as a new type of crystalline porous multifunctional materials, have attracted tremendous interest from scientists in the fields of chemistry and materials science due to their exceptionally high surface area and useful and tunable porosity.[1–3] Meanwhile, the pore surfaces and sizes of metal organic frameworks can be systematically functionalized and varied/tuned because of their diversity in architecture and composition, so MOF materials show rapid development in a variety of application areas, including catalysis,[4] gas storage,[2a,f–h] molecular separation,[2d] drug delivery,[5] and luminescence.[2c] Although numerous MOFs used for storage of small molecule gases have been reported and studied, quite a lot of efforts have been pursued to further enhance their gas adsorption capacity.

To develop microporous metal organic framework materials with high gas adsorption performance, a series of strategies, such as improving the density of metal open sites, increasing the pore volume and surface areas, enhancing the quality of crystals and optimizing the activation conditions, taking advantage of framework catenation and interpenetration, adjusting the pore sizes and modifying the pore surfaces, has been extensively explored.[6] Designing and synthesizing MOFs with open metal sites (OMSs) is one of the best strategies to enhance gas storage properties. The well-known MOF material HKUST-1 (ref. 7) with open copper coordination sites in a large cuboctahedral cage has a high acetylene adsorption capacity of 201 $cm^3\ g^{-1}$. Xiang *et al.*[8] reported a porous material with high densities of open metal sites, CoMOF-74, which exhibits a high volumetric acetylene storage capacity of 230 $cm^3\ cm^{-3}$. However, high densities of open metal sites result in high adsorption enthalpy, which goes against the regeneration of crystal materials. On the other hand, pore size also plays an important role in the aspect of gas adsorption. For promoting the capability of capturing gas molecules, maximizing the guest–framework interaction by matching the pore space with the size of the gas molecules can be identified as an effective approach. To adjust the pore size, several strategies have been reported, such as inserting a symmetry-matching regulated secondary linker or anchoring a metal ion/cluster/functional groups at the cage/channel centers, which make the pore space of the primary framework partition into multiple domains.[6d–j] Zhao *et al.*[6d] introduced a tripyridyl-type linker into a MIL-88-type structure to obtain a family of CPM-33 materials which exhibit superior CO_2 adsorption capacity. In particular, CPM-33b shows the highest CO_2 adsorption value of 126.4 $cm^3\ g^{-1}$ among MOFs without OMSs and is comparable to ZnMOF-74 and NiMOF-74.[2b,9] Herein, with the purpose of improving the gas uptake capacity, we substitute benzene with dimethoxynaphthalene into terphenyl-3,3′,5,5′-tetracarboxylic acid to obtain a new tetracarboxylic organic linker H_4DTPD (Scheme 1) and its corresponding first microporous MOF, $[Cu_2(DTPD)(H_2O)_2]\cdot(DMF)_5\cdot(H_2O)_2$ (**ZJU-12**; H_4DTPD = 5,5′-(2,6-dimethoxynaphthalene-1,5-diyl)diisophthalic acid, ZJU = Zhejiang University), with optimized pore space and open metal sites. The activated **ZJU-12a** exhibits a moderately high BET (Brunauer–Emmett–Teller) surface area of 2316 $m^2\ g^{-1}$ and a

[a] *College of Materials & Environmental Engineering, Hangzhou Dianzi University, Hangzhou, 310027, PR China. E-mail: star1987@hdu.edu.cn*
[b] *State Key Laboratory of Silicon Materials, Cyrus Tang Center for Sensor Materials and Applications, School of Materials Science and Engineering, Zhejiang University, Hangzhou, 310027, PR China. E-mail: gdqian@zju.edu.cn*

† Electronic supplementary information (ESI) available. CCDC 1510153. For ESI and crystallographic data in CIF or other electronic format see DOI: 10.1039/c6ce02291j

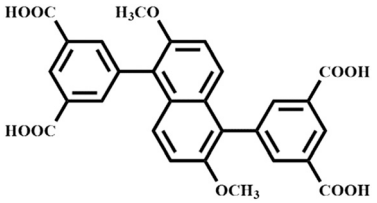

Scheme 1 The organic linker H_4DTPD for the construction of **ZJU-12**.

high C_2H_2 storage capacity of 244 cm^3 g^{-1} and CO_2 capture capacity of 134 cm^3 g^{-1} at room temperature.

Experimental

Synthesis of the organic linker

H_4DTPD was synthesized as shown in Scheme 2.

Dimethyl 5-amino-isophthalate (50 g) was added to 15% hydrobromic acid (900 mL) and cooled to 0 °C. A sodium nitrite solution (2.5 M, 120 mL) was added slowly with stirring to obtain a solution of diazonium bromide. The solution of diazonium bromide was slowly added to a solution including CuBr (49 g) and 15% hydrobromic acid (450 mL) under stirring, while the temperature was always kept under 0 °C. The mixture was kept stirring under room temperature overnight after the addition was completed. The solution was filtered, and the filter cake was dissolved in CCl_2H_2, dried with $MgSO_4$, filtered and concentrated in a vacuum. The crude product was purified by column chromatography (silica gel, ethyl acetate/petroleum ether, 1 : 8 v/v) to obtain dimethyl 5-bromobenzene-1,3-dicarboxylate as a white powder. Yield: 85%. ^{1}H-NMR (500 MHz, $CDCl_3$): δ = 3.95 (s, 6H), 8.35 (d, 2H), 8.61 (s, 1H) ppm.

The dimethyl 5-bromobenzene-1,3-dicarboxylate (5.4 g), bis(pinacolato)diborane (6.0 g), $Pd(dppf)_2Cl_2$ (0.2 g) and potassium acetate (5.6 g) were added to 100 mL of dried 1,4-dioxane. The mixture was kept at 70 °C for 24 h under stirring. Afterwards, the resultant mixture was extracted with 50 mL of ethyl acetate. The organic layer was separated and dried with anhydrous $MgSO_4$. Then, the solvent was concentrated in a vacuum after filtration. Finally, the crude product was purified by column chromatography (silica gel, ethyl acetate/petroleum ether, 1 : 8 v/v) to obtain pure dimethyl (5-pinacolboryl)isophthalate. Yield: 66%. ^{1}H NMR (500 MHz, $CDCl_3$): δ = 1.37 (m, 12H), 3.95 (s, 6H), 8.64 (d, 2H), 8.76 (s, 1H) ppm.

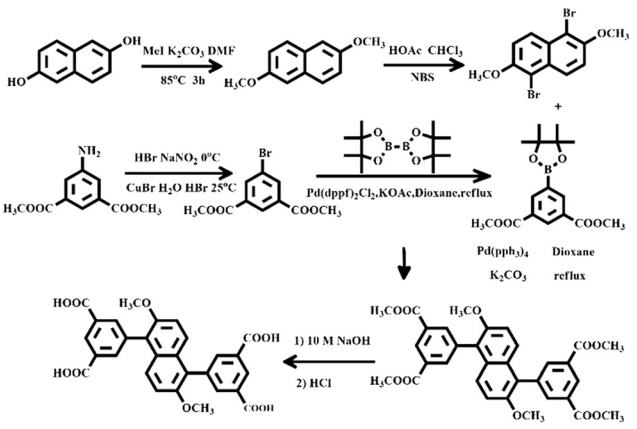

Scheme 2 Synthetic route to the organic linker used to construct **ZJU-12**.

Naphthalene-2,6-diol (10 g) and K_2CO_3 (20 g) were dissolved in DMF (50 mL), then iodomethane (10 mL) was added, and the mixture was kept under 85 °C for 3 hours and afterwards was filtered after adding water (100 mL). The crude product was purified *via* recrystallization of CCl_2H_2 to obtain 2,6-dimethoxynaphthalene. Yield: 85%. ^{1}H NMR (500 MHz, $CDCl_3$): δ = 3.90 (s, 6H), 7.66 (d, 2H), 7.12 (s, 2H), 7.15 (d, 2H) ppm.

A solution of 2,6-dimethoxynaphthalene (5 g) in a 100 mL mixed solvent of $CHCl_3$ and acetic acid (1 : 1) was added to NBS (9.6 g) under 0 °C. After the mixture reacted overnight at room temperature, the mixture was filtered. The solid was washed with water, saturated $NaHCO_3$ solution, ethanol and $CHCl_3$ to afford 1,5-dibromo-2,6-dimethoxynaphthalene as a white solid. Yield: 87%. ^{1}H NMR (500 MHz, $CDCl_3$): δ = 4.04 (s, 6H), 8.26 (d, 2H), 7.37 (d, 2H) ppm.

1,5-Dibromo-2,6-dimethoxynaphthalene (3 g), dimethyl (5-pinacolboryl)isophthalate (5.57 g) and K_2CO_3 (8 g) were added to 100 mL of anhydrous 1,4-dioxane, and the solution was deaerated under Ar for 15 min. $Pd(PPh_3)_4$ (0.47 g) was added to the reaction mixture with stirring, and the mixture was heated to 80 °C for 3 days under Ar. Afterwards, it was extracted with trichloromethane (150 mL). The organic layer was separated and was dried with anhydrous $MgSO_4$ and the solvent was removed in a vacuum. The crude product was purified by column chromatography to obtain tetramethyl 5,5′-(2,6-dimethoxynaphthalene-1,5-diyl)diisophthalate. Yield: 59.2%. ^{1}H-NMR (500 MHz, $CDCl_3$): δ = 3.77 (s, 6H), 3.96 (s, 12H), 8.27 (s, 4H), 8.77 (s, 2H), 7.24 (d, 2H), 7.43 (d, 2H) ppm.

Tetramethyl 5,5′-(2,6-dimethoxynaphthalene-1,5-diyl)-diisophthalate (5 g) was then suspended in 150 mL of NaOH (13.9 g) aqueous solution, and 1,4-dioxane (40 mL) was added. The mixture was stirred under reflux until clarification. Dilute HCl was added to the aqueous solution until the pH of the solution was 2. The solid was collected by filtration, washed with a lot of water, and dried to give 5,5′-(2,6-dimethoxynaphthalene-1,5-diyl)diisophthalic acid (H_4DTPD, 96.7% yield). ^{1}H-NMR (500 MHz, DMSO): δ = 3.76 (s, 6H), 7.38 (d, 2H), 7.50 (d, 2H), 8.09 (s, 4H), 8.56 (s, 2H), 13.39 (s, 4H) ppm.

Synthesis of ZJU-12

In a 20 ml glass vial, the organic linker H_4DTPD (10 mg, 0.0194 mmol) was dissolved in 12.85 mL of *N*,*N*-dimethyl formamide (DMF). Then, $Cu(NO_3)_2{\cdot}2.5H_2O$ (20 mg, 0.086 mmol) and 2.15 mL of H_2O were added into the vial, followed by 75 μL of HCl (37%, aq.). The glass vial was capped and placed in a precision oven at 80 °C for 3 days. Green rhombic shaped crystals were obtained after cooling to room

temperature and washed with DMF three times to afford **ZJU-12**. Elemental analysis: calcd for $[Cu_2(C_{28}H_{16}O_{10})(H_2O)_2]\cdot(DMF)_5\cdot(H_2O)_2$ ($C_{43}H_{59}Cu_2N_5O_{19}$, %): C, 48.04; H, 5.36; N, 6.52; found: C, 48.075; H, 5.564; N, 6.707.

Gas sorption measurements

A Micromeritics ASAP 2020 surface area analyzer was used to measure gas sorption isotherms. To obtain a guest-free framework, the fresh as-synthesized sample of **ZJU-12** was washed with DMF, guest-exchanged with dry acetone at least 10 times, filtered and vacuumed at room temperature for 24 h and then at 383 K until the outgas rate was 5 μmHg min^{-1} prior to measurements. An activated sample of **ZJU-12** (100–120 mg) was used for the sorption measurements. The N_2 sorption measurement was maintained at 77 K with liquid nitrogen. The C_2H_2 and CO_2 sorption measurements were performed at 273 K with an ice-water bath and at 298 K with a water bath.

Results and discussion

The organic ligand H_4DTPD was successfully synthesized by addition reaction and Suzuki cross-coupling followed by hydrolysis of the ester and acidification. **ZJU-12** was obtained by the solvothermal reaction of H_4DTPD and $Cu(NO_3)_2\cdot2.5H_2O$ in DMF/H_2O with addition of a small quantity of HCl at 80 °C for 3 days as blue rhombic shaped crystals. The formulae of **ZJU-12** were confirmed by single-crystal X-ray diffraction studies, elemental analyses and thermogravimetric analysis (TGA, Fig. S1†). The consistency of the powder X-ray diffraction (PXRD) pattern of the as-synthesized samples with the simulated pattern from single-crystal data demonstrates the phase purity of the bulk crystal materials (Fig. S2†).

The single crystal X-ray crystallography (SXRD) analysis proved that **ZJU-12** crystallizes in the trigonal space group $R\bar{3}m$. As expected, **ZJU-12** is built from paddle-wheel $Cu_2(COO)_4$ secondary building units (SBUs) connected to H_4-DTPD linkers *via* carboxylate groups to have the well-known NbO topology (Fig. 1). The 3D framework of **ZJU-12** has two types of cages along the *c* axis. The diameter of the spherical-like cage is about 6.4 Å, taking into account the van der Waals radii (Fig. 1a). Furthermore, the size of the irregular shuttle-shaped cage is approximately 3.2 × 20.6 $Å^2$ (Fig. 1b). The kinetic diameter and molecular dimensional size of C_2H_2 (3.3 Å, 3.32 × 3.34 × 5.7 $Å^3$) and CO_2 (3.3 Å, 3.18 × 3.33 × 5.36 $Å^3$) are a little lower than those of the cages, therefore these two gases can easily enter the cages of the crystal. Furthermore, due to the introduction of dimethoxy-naphthalene, there are smaller sizes of windows along the *a*, *b* and *c* axes in **ZJU-12** materials compared with the prototype framework NOTT-101. One, which has a value of about 1 Å, can be observed along the *c* axis (Fig. 1c) and the other two along the *a* axis are about 2 Å and 2.8 × 5.6 $Å^2$ (Fig. 1d). The smaller window sizes can effectively prevent gas molecules from escaping from the pore space of framework materials. The calculated accessible free pore volume of **ZJU-12a** is

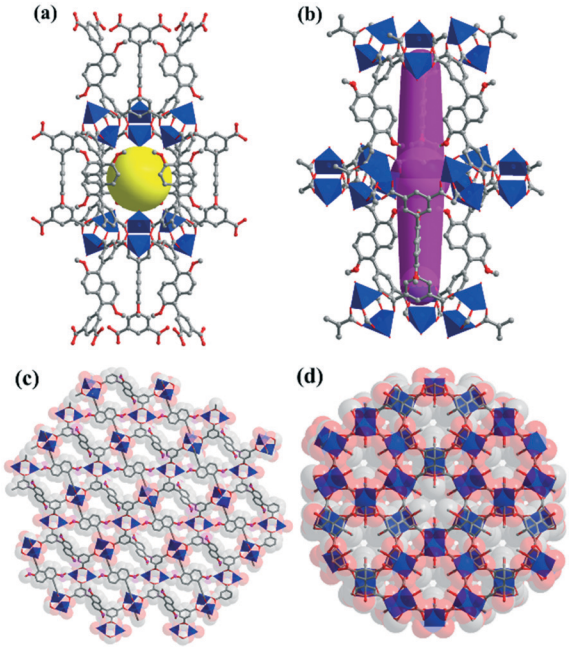

Fig. 1 X-ray single crystal structure of **ZJU-12**, indicating (a) a spherical-like cage of about 6.4 Å in diameter and (b) a shuttle-shaped cage of about 3.2 × 20.6 $Å^2$ (Cu, blue; C: gray; O: red); (c) the structure viewed along the *a* axis indicating the window of about 2 Å and 2.8 × 5.6 $Å^2$, respectively; (d) the structure viewed along the *c* axis showing the window of about 1 Å.

62% (7414 $Å^3$ out of 11 960.5 $Å^3$), evaluated by the PLATON program.[10]

To estimate the permanent porosity, the dry acetone-exchanged **ZJU-12** was activated under high vacuum to obtain the desolvated **ZJU-12a**. The N_2 adsorption isotherm of **ZJU-12a**, which exhibits reversible type-I adsorption behaviour, was acquired at 77 K. The highest adsorbed amount of N_2 for **ZJU-12a** is 606 $cm^3\ g^{-1}$ and the corresponding pore volume is 0.938 $cm^3\ g^{-1}$ (Fig. 2). The surface areas of **ZJU-12a** are evaluated to be 2316 $m^2\ g^{-1}$ from Brunauer–Emmett–Teller (BET) (Fig. S3†) and 2567 $m^2\ g^{-1}$ from Langmuir surface areas. The

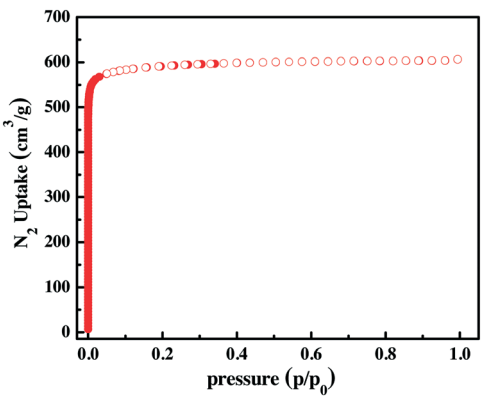

Fig. 2 N_2 sorption isotherm of **ZJU-12a** at 77 K. Solid and open symbols represent adsorption and desorption, respectively.

BET value is slightly lower than that for NOTT-101 (ref. 11*a*) (2805 m^2 g^{-1}) because of substitution of benzene with dimethoxynaphthalene, but is comparable to those for ZJU-25a[11*b*] (2124 m^2 g^{-1}), NOTT-109 (ref. 11*a*) (2110 m^2 g^{-1}), NJU-Bai-14 (ref. 11*c*) (2384 m^2 g^{-1}), ZJNU-54a[11*d*] (2134 m^2 g^{-1}) and ZJNU-44 (ref. 11*e*) (2314 m^2 g^{-1}). The pore size distribution calculated by the Horvath–Kawazoe model is in the range from 4 Å to 6 Å, which is consistent with the pore sizes from SXRD (Fig. S4†).

Acetylene is one of the important raw materials in industrial production, but the storage of acetylene is required to be under suitable low pressure, otherwise it has the possibility of explosion. Among all kinds of porous materials, MOF materials are considered to be the most promising ones for such an application. The optimized pore space and open metal sites within the framework of **ZJU-12a** encourage us to study its adsorption performance for acetylene and methane. We examine the acetylene adsorption of **ZJU-12a**. As shown in Fig. 3a, **ZJU-12a** can take up a large amount of acetylene. At 273 K and 298 K, the acetylene saturated adsorption capacity of **ZJU-12a** can reach 301 cm^3 g^{-1} and 244 cm^3 g^{-1}, respectively. The gravimetric acetylene storage capacity of **ZJU-12a** at room temperature is significantly higher than those of examined porous MOF materials.[2*f*,7,12] In fact, the gravimetric C_2H_2 adsorption capacity of 244 cm^3 g^{-1} is the highest one ever reported (Table 1), indicating the promise of this novel microporous MOF material for practical acetylene storage applications. Taking the framework density of 0.799 g cm^{-3} without the coordinated waters into account, the volumetric capacities are 241 cm^3 cm^{-3} and 195 cm^3 cm^{-3} at 273 K and 298 K, respectively. The initial Q_{st} of C_2H_2 adsorption in **ZJU-12a** is calculated to be 29 kJ mol^{-1} (Fig. 4), which is significantly lower than that for MOF-74 with high densities of open metal sites.

Table 1 Comparison of C_2H_2 uptake in porous MOFs

MOFs	S_{BET} (m^2 g^{-1})	V_P (cm^3 g^{-1})	C_2H_2 uptake (cm^3 g^{-1})	Ref.
ZJU-12a	2316	0.938	244	This work
FJI-H8	2025	0.82	224	12*e*
NJU-Bai17	2423	0.914	222.4	12*g*
ZJU-40a	2858	1.06	216	12*o*
ZJNU-47	2638	1.031	213	12*h*
ZJNU-54	2134	0.871	211	11*d*
Cu_2TPTC-OMe	2278	1.039	204	12*j*
Cu_2TPTC-Me	2405	0.9805	203	12*j*
HKUST-1	1850	0.76	201	7
CoMOF-74	1504	0.63	197	12*b*
ZJU-8a	2501	1.0224	195	12*k*
ZJU-5a	2823	1.074	193	12*f*
ZJU-9a	2353	0.887	193	12*l*
ZJU-70	1362	0.676	191	12*c*
NOTT-101	2805	1.080	184	12*d*
ZJU-7a	2198	0.8945	180	12*m*
PCN-16	2810	1.06	176	12*a*
MOF-505	1139	0.67	148	7
NOTT-102	3342	1.280	146	12*d*
ZJU-26a	989	0.572	84	12*n*

The excessive emission of carbon dioxide (CO_2) is the major factor for the greenhouse effect. MOF materials are very promising solid porous adsorbents for CO_2 capture on account of their intrinsic advantages. We investigate the CO_2 adsorption performance, indicating that **ZJU-12a** exhibits a CO_2 uptake of 243 cm^3 g^{-1} at 273 K and 134 cm^3 g^{-1} at 298 K at 1 bar (Fig. 3b). Remarkably, the gravimetric CO_2 sorption capacity at room temperature is higher than those of MOF materials ZJNU-54a[12*i*] (120 cm^3 g^{-1}), PCN-124 (ref. 13*a*) (114 cm^3 g^{-1}), ZJNU-44 (ref. 13*b*) (116 cm^3 g^{-1}), NPC-6 (ref. 13*c*)

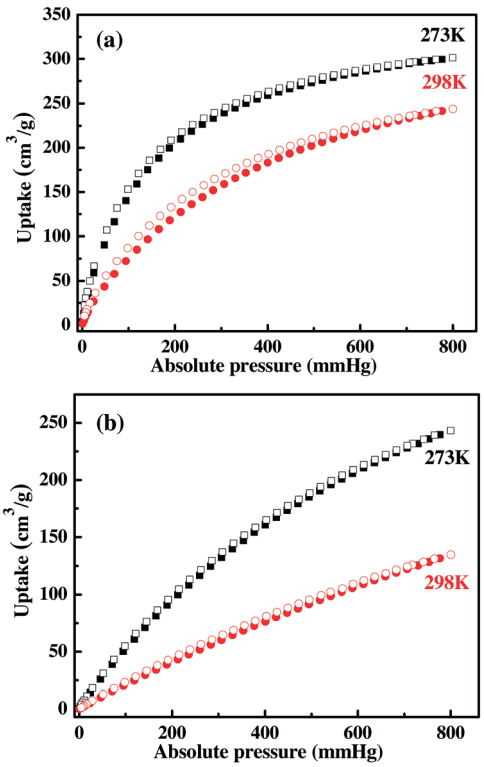

Fig. 3 Gas sorption isotherms of **ZJU-12a** for (a) C_2H_2 at 273 K and 298 K, and (b) CO_2 at 273 K and 298 K. Solid symbols: adsorption, open symbols: desorption.

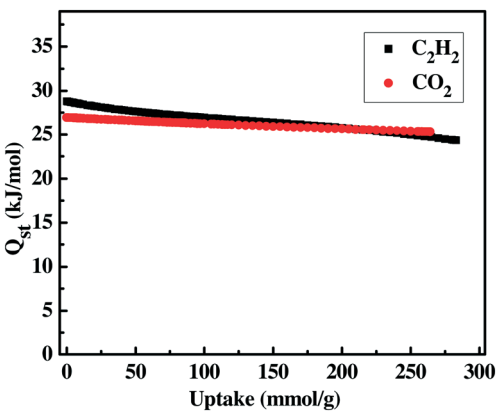

Fig. 4 The isosteric heats of adsorption of C_2H_2 and CO_2 calculated using the virial method.

(108 cm^3 g^{-1}), JLU-Liu21 (ref. 13*d*) (118 cm^3 g^{-1}), NJU-Bai21 (ref. 13*e*) (115 cm^3 g^{-1}) and NJU-Bai-14 (ref. 11*c*) (100 cm^3 g^{-1}). The high C_2H_2 and CO_2 adsorption values demonstrate that open metal sites and optimized pore size can really enhance the interaction between the gas molecules and the framework. The initial adsorption enthalpy Q_{st} for CO_2 was calculated by the virial method and the value is 26.9 kJ mol^{-1} (Fig. 4). Such low C_2H_2 and CO_2 adsorption enthalpy values meet the requirement of low energy consumption in the adsorbent recycling process.

Conclusions

In summary, by substituting benzene with dimethoxynaphthalene within the framework, we have developed a three-dimensional microporous metal–organic framework, **ZJU-12**. The activated **ZJU-12a** exhibits a moderately high BET surface area of 2316 m^2 g^{-1}. The optimized pore space and open metal sites within **ZJU-12a** have enabled this novel framework material to adsorb a large amount of C_2H_2 (244 cm^3 g^{-1}) and CO_2 (134 cm^3 g^{-1}) at room temperature. Thus, this new MOF can be a promising adsorbent for gas storage applications.

Acknowledgements

The authors gratefully acknowledge financial support from the National Natural Science Foundation of China (No. 51472217, 51432001 and 51602087) and the Zhejiang Provincial Natural Science Foundation of China (No. LZ15E020001).

Notes and references

1 (*a*) M. Eddaoudi, J. Kim, N. Rosi, D. Vodak, J. Wachter, M. O'Keeffe and O. M. Yaghi, *Science*, 2002, **295**, 469–472; (*b*) M. P. Suh, H. J. Park, T. K. Prasad and D.-W. Lim, *Chem. Rev.*, 2012, **112**, 782–835; (*c*) H. Furukawa, N. Ko, Y. B. Go, N. Aratani, S. B. Choi, E. Choi, A. Ö. Yazaydin, R. Q. Snurr, M. O'Keeffe, J. Kim and O. M. Yaghi, *Science*, 2010, **329**, 424–428; (*d*) E. D. Bloch, W. L. Queen, R. Krishna, J. M. Zadrozny, C. M. Brown and J. R. Long, *Science*, 2012, **335**, 1606–1610; (*e*) J.-R. Li, J. Sculley and H.-C. Zhou, *Chem. Rev.*, 2012, **112**, 869–932; (*f*) S. S.-Y. Chui, S. M.-F. Lo, J. P. H. Charmant, A. G. Orpen and I. D. Williams, *Science*, 1999, **283**, 1148–1150; (*g*) B. Chen, M. Eddaoudi, S. T. Hyde, M. O'Keeffe and O. M. Yaghi, *Science*, 2001, **291**, 1021–1023.

2 (*a*) Y. He, W. Zhou, G. Qian and B. Chen, *Chem. Soc. Rev.*, 2014, **43**, 5657–5678; (*b*) K. Sumida, D. L. Rogow, J. A. Mason, T. M. McDonald, E. D. Bloch, Z. R. Herm, T.-H. Bae and J. R. Long, *Chem. Rev.*, 2012, **112**, 724–781; (*c*) Y. Cui, Y. Yue, G. Qian and B. Chen, *Chem. Rev.*, 2012, **112**, 1126–1162; (*d*) B. Li, H. Wang and B. Chen, *Chem. – Asian J.*, 2014, **9**, 1474–1498; (*e*) H.-L. Jiang, T. A. Makal and H.-C. Zhou, *Coord. Chem. Rev.*, 2013, **257**, 2232–2249; (*f*) Z. Zhang, S. Xiang and B. Chen, *CrystEngComm*, 2011, **13**, 5983–5992; (*g*) Z. Zhang, Z.-Z. Yao, S. Xiang and B. Chen, *Energy Environ. Sci.*, 2014, **7**, 2868–2899; (*h*) Y. He, W. Zhou, R. Krishna and B. Chen, *Chem. Commun.*, 2012, **48**, 11813–11831; (*i*) Y. Bai, Y. Dou, L.-H. Xie, W. Rutledge, J.-R. Li and H.-C. Zhou, *Chem. Soc. Rev.*, 2016, **45**, 2327–2367; (*j*) W. Lu, Z. Wei, Z. Gu, T. Liu, J. Park, J. Park, J. Tian, M. Zhang, Q. Zhang, T. Gentle III, M. Bosch and H. C. Zhou, *Chem. Soc. Rev.*, 2014, **43**, 5561–5593.

3 (*a*) T. M. McDonald, J. A. Mason, X. Kong, E. D. Bloch, D. Gygi, A. Dani, V. Crocella, F. Giordanino, S. O. Odoh, W. S. Drisdell, B. Vlaisavljevich, A. L. Dzubak, R. Poloni, S. K. Schnell, N. Planas, K. Lee, T. Pascal, L. F. Wan, D. Prendergast, J. B. Neaton, B. Smit, J. B. Kortright, L. Gagliardi, S. Bordiga, J. A. Reimer and J. R. Long, *Nature*, 2015, **519**, 303–308; (*b*) K. Koh, A. G. Wong-Foy and A. J. Matzger, *J. Am. Chem. Soc.*, 2009, **131**, 4184–4185; (*c*) Y.-X. Tan, Y.-P. He and J. Zhang, *RSC Adv.*, 2015, **5**, 7794–7797; (*d*) S. Yang, X. Lin, W. Lewis, M. Suyetin, E. Bichoutskaia, J. E. Parker, C. C. Tang, D. R. Allan, P. J. Rizkallah, P. Hubberstey, N. R. Champness, K. Mark Thomas, A. J. Blake and M. Schröder, *Nat. Mater.*, 2012, **11**, 710–716; (*e*) H. Wu, W. Zhou and T. Yildirim, *J. Am. Chem. Soc.*, 2009, **131**, 4995–5000; (*f*) T.-L. Hu, H. Wang, B. Li, R. Krishna, H. Wu, W. Zhou, Y. Zhao, Y. Han, X. Wang, W. Zhu, Z. Yao, S. Xiang and B. Chen, *Nat. Commun.*, 2015, **6**, 7328–7336; (*g*) J. Jiang, H. Furukawa, Y.-B. Zhang and O. M. Yaghi, *J. Am. Chem. Soc.*, 2016, **138**, 10244–10251; (*h*) Y. Cui, B. Li, H. He, W. Zhou, B. Chen and G. Qian, *Acc. Chem. Res.*, 2016, **49**, 483–493.

4 (*a*) T. Zhang, K. Manna and W. Lin, *J. Am. Chem. Soc.*, 2016, **138**, 3241–3249; (*b*) M. Zhao, S. Ou and C.-D. Wu, *Acc. Chem. Res.*, 2014, **47**, 1199–1207; (*c*) A. Corma, H. Garcia and F. X. Llabrés i Xamena, *Chem. Rev.*, 2010, **110**, 4606–4655; (*d*) A. H. Chughtai, N. Ahmad, H. A. Younus, A. Laypkov and F. Verpoort, *Chem. Soc. Rev.*, 2015, **44**, 6804–6849.

5 (*a*) A. C. McKinlay, R. E. Morris, P. Horcajada, G. Férey, R. Gref, P. Couvreur and C. Serre, *Angew. Chem., Int. Ed.*, 2010, **49**, 6260–6266 (*Angew. Chem.*, 2010, **122**, 6400–6406); (*b*) J. Della Rocca, D. Liu and W. Lin, *Acc. Chem. Res.*, 2011, **44**, 957–968; (*c*) P. Horcajada, R. Gref, T. Baati, G. Maurin, P. Couvreur, G. Ferey, R. E. Morris and C. Serre, *Chem. Rev.*, 2012, **112**, 1232–1268; (*d*) C.-Y. Sun, C. Qin, X.-L. Wang and Z.-M. Su, *Expert Opin. Drug Delivery*, 2013, **10**, 89–101.

6 (*a*) H. K. Chae, D. Y. Siberio-Perez, J. Kim, Y. Go, M. Eddaoudi, A. J. Matzger, M. O'Keeffe and O. M. Yaghi, *Nature*, 2004, **427**, 523–527; (*b*) B. Kesanli, Y. Cui, M. R. Smith, E. W. Bittner, B. C. Bockrath and W. Lin, *Angew. Chem., Int. Ed.*, 2005, **44**, 72–75; (*c*) S. S. Kaye, A. Dailly, O. M. Yaghi and J. R. Long, *J. Am. Chem. Soc.*, 2007, **129**, 14176–14177; (*d*) X. Zhao, X. Bu, Q.-G. Zhai, H. Tran and P. Feng, *J. Am. Chem. Soc.*, 2015, **137**, 1396–1399; (*e*) S.-T. Zheng, J. T. Bu, Y. Li, T. Wu, F. Zuo, P. Feng and X. Bu, *J. Am. Chem. Soc.*, 2010, **132**, 17062–17064; (*f*) S.-T. Zheng, C. Mao, T. Wu, S. Lee, P. Feng and X. Bu, *J. Am. Chem. Soc.*, 2012, **134**, 11936–11939; (*g*) S.-T. Zheng, T. Wu, F. Zuo, C.-T. Chou, P. Feng and X. Bu, *J. Am. Chem. Soc.*, 2012, **134**, 1934–1937; (*h*) F. Bu, Q. Lin, Q. Zhai, L. Wang, T. Wu, S.-T.

Zheng, X. Bu and P. Feng, *Angew. Chem., Int. Ed.*, 2012, **51**, 8538–8541; (*i*) S.-T. Zheng, T. Wu, B. Irfanoglu, F. Zuo, P. Feng and X. Bu, *Angew. Chem., Int. Ed.*, 2011, **50**, 8034–8037; (*j*) S.-T. Zheng, X. Zhao, S. Lau, A. Fuhr, P. Feng and X. Bu, *J. Am. Chem. Soc.*, 2013, **135**, 10270–10273.

7 S. Xiang, W. Zhou, J. M. Gallegos, Y. Liu and B. Chen, *J. Am. Chem. Soc.*, 2009, **131**, 12415–12419.

8 S. Xiang, Y. He, Z. Zhang, H. Wu, W. Zhou, R. Krishna and B. Chen, *Nat. Commun.*, 2012, **3**, 954–962.

9 S. R. Caskey, A. G. Wong-Foy and A. J. Matzger, *J. Am. Chem. Soc.*, 2008, **130**, 10870–10871.

10 L. Spek, *PLATON*, The University of Utrecht, Utrecht, The Netherlands, 1999.

11 (*a*) Y. He, W. Zhou, T. Yildirim and B. Chen, *Energy Environ. Sci.*, 2013, **6**, 2735–2744; (*b*) X. Duan, J. Yu, J. Cai, Y. He, C. Wu, W. Zhou, T. Yildirim, Z. Zhang, S. Xiang, M. O'Keeffe, B. Chen and G. Qian, *Chem. Commun.*, 2013, **49**, 2043–2045; (*c*) M. Zhang, Q. Wang, Z. Lu, H. Liu, W. Liu and J. Bai, *CrystEngComm*, 2014, **16**, 6287–6290; (*d*) J. Jiao, L. Dou, H. Liu, F. Chen, D. Bai, Y. Feng, S. Xiong, D.-L. Chen and Y. He, *Dalton Trans.*, 2016, **45**, 13373–13382; (*e*) C. Song, J. Hu, Y. Ling, Y.-L. Feng, R. Krishna, D.-L. Chen and Y. He, *J. Mater. Chem. A*, 2015, **3**, 19417–19426.

12 (*a*) Y. Hu, S. Xiang, W. Zhang, Z. Zhang, L. Wang, J. Bai and B. Chen, *Chem. Commun.*, 2009, 7551–7553; (*b*) S. Xiang, W. Zhou, Z. Zhang, M. A. Green, Y. Liu and B. Chen, *Angew. Chem., Int. Ed.*, 2010, **49**, 4615–4618; (*c*) X. Duan, C. Wu, S. Xiang, W. Zhou, T. Yildirim, Y. Cui, Y. Yang, B. Chen and G. Qian, *Inorg. Chem.*, 2015, **54**, 4377–4381; (*d*) Y. He, R. Krishna and B. Chen, *Energy Environ. Sci.*, 2012, **5**, 9107–9120; (*e*) J. Pang, F. Jiang, M. Wu, C. Liu, K. Su, W. Lu, D. Yuan and M. Hong, *Nat. Commun.*, 2015, **6**, 7575–7581; (*f*) X. Rao, J. Cai, J. Yu, Y. He, C. Wu, W. Zhou, T. Yildirim, B. Chen and G. Qian, *Chem. Commun.*, 2013, **49**, 6719–6721; (*g*) M. Zhang, B. Li, Y. Li, Q. Wang, W. Zhang, B. Chen, S. Li, Y. Pan, X. You and J. Bai, *Chem. Commun.*, 2016, **52**, 7241–7244; (*h*) C. Song, J. Jiao, Q. Lin, H. Liu and Y. He, *Dalton Trans.*, 2016, **45**, 4563–4569; (*i*) J. Jiao, L. Dou, H. Liu, F. Chen, D. Bai, Y. Feng, S. Xiong, D.-L. Chen and Y. He, *Dalton Trans.*, 2016, **45**, 13373–13382; (*j*) T. Xia, J. Cai, H. Wang, X. Duan, Y. Cui, Y. Yang and G. Qian, *Microporous Mesoporous Mater.*, 2015, **215**, 109–115; (*k*) J. Cai, H. Wang, H. Wang, X. Duan, Z. Wang, Y. Cui, Y. Yang, B. Chen and G. Qian, *RSC Adv.*, 2015, **5**, 77417–77422; (*l*) X. Duan, H. Wang, Y. Cui, Y. Yang, Z. Wang, B. Chen and G. Qian, *RSC Adv.*, 2015, **5**, 84446–84450; (*m*) J. Cai, Y. Lin, J. Yu, C. Wu, L. Chen, Y. Cui, Y. Yang, B. Chen and G. Qian, *RSC Adv.*, 2014, **4**, 49457–49461; (*n*) X. Duan, J. Cai, J. Yu, C. Wu, Y. Cui, Y. Yang and G. Qian, *Microporous Mesoporous Mater.*, 2013, **181**, 99–104; (*o*) H. Wen, H. Wang, B. Li, Y. Cui, H. Wang, G. Qian and B. Chen, *Inorg. Chem.*, 2016, **55**, 7214–7218.

13 (*a*) J. Park, J.-R. Li, Y.-P. Chen, J. Yu, A. A. Yakovenko, Z. U. Wang, L.-B. Sun, P. B. Balbuena and H.-C. Zhou, *Chem. Commun.*, 2012, **48**, 9995–9997; (*b*) C. Song, J. Hu, Y. Ling, Y. Feng, R. Krishna, D.-L. Chen and Y. He, *J. Mater. Chem. A*, 2015, **3**, 19417–19426; (*c*) Q. Mu, H. Wang, L. Li, C. Wang, Y. Wang and X. Zhao, *Chem. – Asian J.*, 2015, **10**, 1864–1869; (*d*) B. Liu, S. Yao, C. Shi, G. Li, Q. Huo and Y. Liu, *Chem. Commun.*, 2016, **52**, 3223–3226; (*e*) Z. Lu, J. Bai, C. Hang, F. Meng, W. Liu, Y. Pan and X. You, *Chem. – Eur. J.*, 2016, **22**, 6277–6285.